Ineffectiveness of energy filtering at grain boundaries for thermoelectric materials

M. Bachmann, M. Czerner, and C. Heiliger*
I. Physikalisches Institut, Justus-Liebig-University Giessen, Giessen, Germany
(Received 25 April 2012; revised manuscript received 20 July 2012; published 13 September 2012)

We use a one-band effective mass model within the Landauer formalism to investigate the influence of double Schottky barriers on the thermoelectric coefficients. It is assumed that these double Schottky barriers arise due to trapping states in grain boundaries. Such barriers can cause an energy filtering effect, which is widely believed to advance thermoelectric efficiencies. We show that for low doping concentrations the Seebeck coefficient is indeed increased due to energy filtering effects, whereas the electric conductivity is strongly decreased. The resulting power factor is also decreased. For higher doping concentrations, which are necessary for large electric conductivities and thus reasonable ZT values, the double Schottky barriers are very small and have therefore an insignificant impact on the thermoelectric parameters. Consequently, there is no significant influence of grain boundaries on ZT values due to additional electrostatic barriers. This does not preclude that other mechanisms at grain boundaries, such as additional scattering due to disorder, can have a positive impact on the power factor.

DOI: 10.1103/PhysRevB.86.115320 PACS number(s): 72.20.Pa, 72.20.Dp, 73.40.−c

I. INTRODUCTION

The maximum efficiency of power conversion in a thermoelectric module is linked to its materials by the figure of merit ZT[1]

$$ZT = \frac{S^2 T \sigma}{\kappa}, \tag{1}$$

where S is the Seebeck coefficient, κ is the thermal conductivity, T is the temperature, and σ is the electric conductivity.

There are different approaches to optimize the figure of merit either by manipulating the electronic structure or by decreasing the thermal conductivity of the phonons without disturbing the transport of the electrons. The latter idea can be summarized by the electron crystal/phonon glass approach.[2] Manipulating the electronic structure mainly aims at the increase of the Seebeck coefficients or on an optimization of the Lorenz number L within the Wiedemann-Franz law

$$\frac{\kappa}{\sigma} = LT. \tag{2}$$

Thereby, one idea is to go to lower dimensions to get peaks in the density of states, which in turn can lead to a higher Seebeck coefficient.[3]

Another idea is the manipulation of the electronic transport properties to increase the Seebeck coefficient and thus the figure of merit. A prominent example of this approach that we want to discuss in this paper is the so-called energy filtering,[1,4–9] where an energy-dependent filtering effect can increase the Seebeck coefficient. The mechanism is that hot electrons can pass an additional barrier whereas cold electrons get blocked at this barrier. Consequently, the Seebeck coefficient is enhanced. Such a filtering effect is reported for indium gallium arsenide superlattice films,[10] bulk PbTe with Pb nanoparticles,[11] nanocrystalline PbTe,[12–14] nanostructured SiGe,[15] and ZnO-based materials.[16–18] An additional advantage that often comes along with such an energy-filtering mechanism is an additional phonon scattering,[10,12,13,19] which reduces the phonon part of the thermal conductivity and therefore can also increase the figure of merit. One drawback of the filtering effect is always a reduction of the electric conductivity.

In this paper we investigate the effect of energy filtering at grain boundaries due to double Schottky barriers. It is widely believed that this effect can enhance the figure of merit in granular systems.[5,9] We show in our paper that this is not true for realistic systems. The origin is that the barrier height and width themselves depend on the number of charge carriers and are vanishing for a reasonably high number of charge carriers. To describe the double Schottky barrier at grain boundaries we use the model by Seto.[20] Although the model was first used to describe polycrystalline silicon it has been successfully used for many different material systems.[21,22] The model works for n- and p-type materials. Other groups also use this model to explain the thermoelectric behavior of different materials.[5,23]

The basic idea of this model is the assumption of additional surface states. For an n-type semiconductor these states can be filled by electrons from donor levels. This will lead to a negative space charge region directly at the interface and to positive space charge regions on both sides of the interface. These space charge regions create a so-called double Schottky barrier that acts as a barrier for electrons. A schematic sketch of the band structure in real space is shown in Fig. 1. The grains are characterized by their length l_g, the length of the interface region l_i, the density of the surface states N_T, the energy levels of the trapping states E_T, the donor density N_D, and the energy levels of the donors E_D. The electrons in the donor states pass over into the deep surface states, which arise in the grain boundary. This leads to a negative charge accumulation in the grain boundaries and to a positive charge accumulation in the vicinity of the grain boundaries. The resulting space charge distribution then creates a so-called double Schottky barrier. In the following we describe the steps to get a quantitative description of the double Schottky barrier. First we choose l_g, l_i, N_T, and N_D. The negative space charge density in the boundary region is N_T. The positive space charge density is N_D and the length of the positive space charge region, which we call screening length l_{scr}, is chosen such that the total charge in the grain is zero $l_{\mathrm{scr}} = \frac{l_i N_T}{N_D}$. Once we obtain the space charge density $n(x)$, we use the Poisson equation to get the potential profile $V(x)$. We assume a constant dielectric permittivity ϵ_r throughout the whole grain.

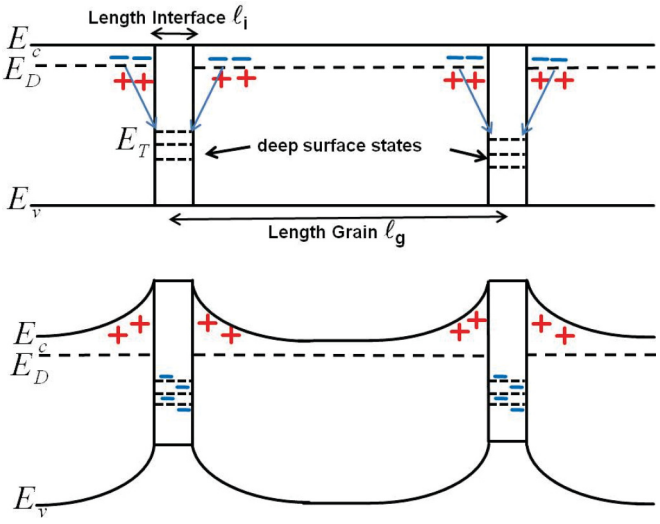

FIG. 1. (Color online) Schematic band diagram in real space before (top) and after (bottom) the generation of the double Schottky barrier. E_c is the energy at the bottom of the conduction band and E_v is the top of the valence band.

In Fig. 2 (top), the space charge distribution and the resulting double Schottky barrier for the parameters $l_i = 0.5$nm, $N_T = 1 \times 10^{20}\text{cm}^{-3}$, $N_D = 1 \times 10^{19}\text{cm}^{-3}$, and $\epsilon_r = 10$ are shown. Double Schottky barriers for different donor densities are shown in bottom panel of Fig. 2. The height and the width of the barriers decrease strongly with increasing donor density.

II. METHOD

For the determination of the chemical potential we consider three kinds of states in our system. The deepest states are in the boundary. There are $N_T l_i$ total states of this kind per grain at energy E_T. The next higher states in energy are the donor states. There are $N_D l_g$ total donor states per grain at energy

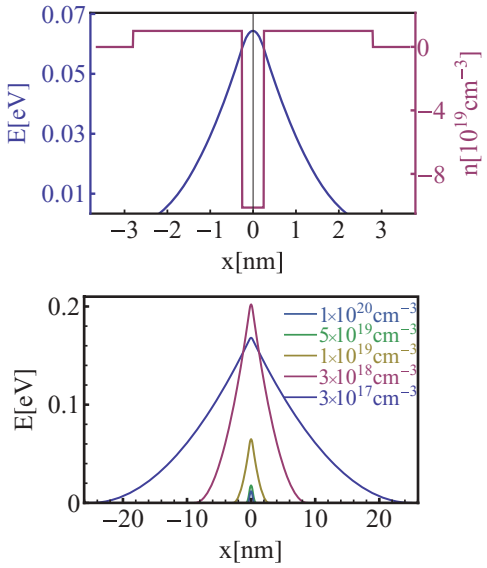

FIG. 2. (Color online) Top: Space charge distribution (red) and the corresponding potential profile (blue) around the interface. Bottom: double Schottky barrier for different donor densities.

E_D. For the remaining states we choose the density of states of a single band with a parabolic dispersion. We determine the value of the chemical potential μ at a given temperature T by imposing charge neutrality. This way, the chemical potential ensures that the number of ionized donors equals the number of electrons trapped in the boundary region plus the number of electrons in the conduction band.

We use the nonequilibrium Green's function (NEGF) method[24–27] to calculate ballistic transport through a double Schottky barrier. The Green's function of the system is given by

$$G(E) = (E - H - \Sigma_l - \Sigma_r)^{-1}, \tag{3}$$

where H is the one-band effective mass Hamiltonian, Σ_l and Σ_r are the self-energies of the semi-infinite leads, and E is the energy. The one-dimensional transmission probability is given by

$$T_{1D}(E) = \text{Tr}[\Gamma_l(E)G(E)\Gamma_r(E)G(E)^\dagger], \tag{4}$$

where Γ_l and Γ_r are the imaginary parts of the left and right self-energies, respectively. The transmission function through the barrier in three dimensions can be obtained by integration over the Brillouin zone

$$\overline{T}_{\text{Bar}}(E) = \frac{L_x L_y m_{\text{eff}}}{2\pi\hbar^2} E2 \int_0^1 dx x T_{1D}(Ex^2). \tag{5}$$

According to Ref. 28 the transmission function $\overline{T}_{\text{Bar}}$ can be divided into

$$\overline{T}_{\text{Bar}}(E) = M(E) T_{\text{Bar}}(E), \tag{6}$$

where

$$M(E) = \frac{L_x L_y m_{\text{eff}}}{2\pi\hbar^2} E \tag{7}$$

is the number of modes and $T_{\text{Bar}}(E)$ is the average transmission probability per carrier at energy E

$$T_{\text{Bar}}(E) = 2 \int_0^1 dx x T_{1D}(Ex^2). \tag{8}$$

In addition to scattering at the grain boundary, electrons are also affected by other scattering mechanisms such as phonon scattering or scattering at impurities. To handle these scattering mechanism we define a second transmission function T_{Bulk}. T_{Bulk} can be written as[25]

$$T_{\text{Bulk}} = \frac{\lambda}{l_g + \lambda}, \tag{9}$$

where λ has the form[28]

$$\lambda = \lambda_0 (E/k_B T)^r. \tag{10}$$

λ_0 is a constant, l_g is the length of the grain, and r specifies the kind of scattering. The different scattering mechanisms T_{Bulk} and T_{Bar} can be combined incoherently by using[25]

$$T_{\text{Grain}}(E) = \frac{1}{1/T_{\text{Bulk}} + 1/T_{\text{Bar}} - 1}. \tag{11}$$

$T_{\text{Grain}}(E)$ is the transmission function of one grain. Since we want to describe a macroscopic solid, we consider n grains in series. The incoherently combined transmission function of

n scatterers in series can be calculated using again Eq. (11) to obtain

$$T_{\text{Solid}}(E) = \frac{1}{n}\frac{T_{\text{Grain}}}{1 - T_{\text{Grain}} + \frac{T_{\text{Grain}}}{n}}. \tag{12}$$

For n we can write $\frac{L}{l_g}$, where L is the length of the sample, and hence

$$T_{\text{Solid}}(E) = \frac{l_g}{L}\frac{T_{\text{Grain}}}{1 - T_{\text{Grain}} + \frac{T_{\text{Grain}} l_g}{L}}, \tag{13}$$

where the term $\frac{T_{\text{Grain}} l_g}{L}$ describes the contact conductance of the sample. For $T_{\text{Grain}} < 1$ and $l_g \ll L$ the contact conductance is negligible and the grain conductance dominates.

Using Onsager relations in linear response the thermoelectric coefficients can be linked to the transmission function $\overline{T}_{\text{Solid}}(E) = M(E)T_{\text{Solid}}(E)$ within the Landauer formalism by the following equations[29]

$$\sigma = e^2 L_0, \tag{14a}$$

$$S = -\frac{1}{eT}\frac{L_1}{L_0}, \tag{14b}$$

$$\kappa_e = \frac{1}{T}\left(L_2 - \frac{L_1^2}{L_0}\right), \tag{14c}$$

$$L_j = \frac{2}{h}\int_{-\infty}^{\infty} \overline{T}_{\text{Solid}}(E)(E-\mu)^j \left(-\frac{\partial f}{\partial E}\right) dE. \tag{14d}$$

At this point we want to stress that even though we are using the Landauer formalism this does not mean that the transport description is purely ballistic. The transport in the grain is assumed to be diffusive and described by Eqs. (9) and (10), whereas the transport across the grain boundary is described as ballistic. Although the formalism used by other groups is different, the physical description of the problem is in principle the same. For instance Popescu *et al.*[9] also use a diffusive description for the transport in the grains and a ballistic description for the grain boundaries. The central quantity in their formalism is the scattering time $\tau(E)$, whereas in our formalism the central quantity is the transmission function $T(E)$. However, in principle both formalisms describe the same physics, their relation is shown in Ref. 28.

III. RESULTS

A. Simple model

We first investigate the effect of energy filtering within a more general framework. Since in our complex model the barrier height and width depend on N_T and N_D, which also influence the chemical potential, we first employ a simpler model for the barrier transmission. From the results obtained with the simple model we can estimate the conditions under which the thermoelectric efficiency can be increased. In the next step we investigate if these conditions can be fulfilled in a more realistic model.

To estimate the highest enhancement caused by energy filtering due to a barrier we choose a step function for the transmission function $T_{1\text{D}}(E)$

$$T_{1\text{D}}(E) = \begin{cases} 1 & E > U_b \\ 0 & E \leqslant U_b \end{cases}. \tag{15}$$

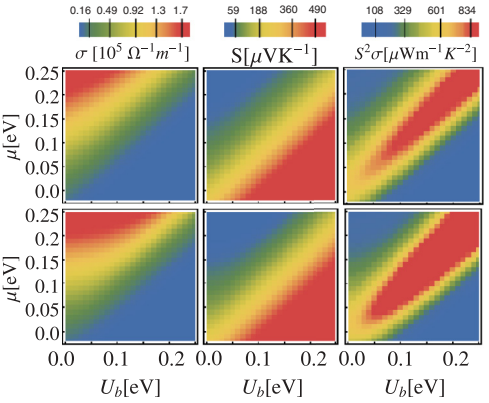

FIG. 3. (Color online) Electric conductivity σ, Seebeck coefficient S, and power factor $S^2\sigma$ vs chemical potential μ and barrier height U_b for different grain sizes l_g. Top: $l_g = 50$ nm. Bottom: $l_g = 200$ nm.

For our investigation we use an effective mass and a constant value for λ to omit additional energy filtering due to scattering effects other than the barrier. With these assumptions we obtain the following expression for the transmission function $\overline{T}_{\text{Solid}}$:

$$\overline{T}_{\text{Solid}}(E) = \begin{cases} \frac{m_{\text{eff}}}{2\pi\hbar^2} E \frac{\lambda(E-U_b)l_g}{El_g + U_b(\lambda - l_g)} & E > U_b \\ 0 & E \leqslant U_b \end{cases}. \tag{16}$$

Figure 3 shows the thermoelectric coefficients vs barrier height and chemical potential for different grain sizes. The following parameters were used: $m_{\text{eff}} = 0.25 \times m_0$, $\lambda_0 = 20$ nm, $r = 0$, and $T = 300$ K. These parameters describe a typical semiconductor and are used to make general statements. A few general trends can be seen. The conductivity increases with increasing chemical potential and decreases with increasing barrier height. The Seebeck coefficient shows the opposite behavior. For a given chemical potential the power factor has a maximum when the barrier height is close to the chemical potential. To conclude this part we emphasize that with a constant barrier it is indeed possible to optimize the power factor as shown in Ref. 9. However, we will show in the following that the barrier itself depends on the chemical potential and the above criteria cannot be fulfilled. Therefore, no significant increase in the power factor is possible.

B. Realistic model

We just showed under what conditions the power factor can be increased due to a barrier. In principle, one needs a high chemical potential and a barrier height that is in the range of the chemical potential. For the real system we run into difficulties, since a high chemical potential requires a high donor density, which leads to an effective screening of the Coulomb potential, which in turn reduces the height and the width of the double Schottky barrier. This reduces the effect of the energy filtering.

To make quantitative judgments we calculate the thermoelectric coefficients for different chemical potentials and different barriers by altering the density of the surface states N_T from 0 to 2×10^{20} cm^{-3}. Since the interface thickness is 1 nm, this corresponds to a total trapped charge density Q_T of 2×10^{13} cm^{-2}. Hence the range of N_T covers typical values for Q_T.[20] For the other parameters we used typical

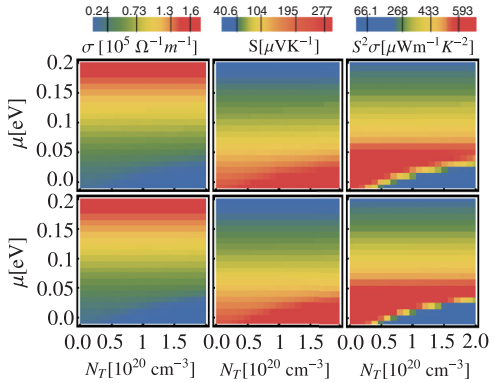

FIG. 4. (Color online) Electric conductivity σ, Seebeck coefficient S, and power factor $S^2\sigma$ vs chemical potential μ and density of the surface states N_T for different grain sizes l_g. Top: $l_g = 50$ nm. Bottom: $l_g = 200$ nm.

values ($E_D = -20$ meV, $E_T = -500$ meV, $l_i = 1$ nm, $m_{\text{eff}} = 0.25 \times m_0$, $\epsilon_r = 10$, $\lambda_0 = 20$ nm, $r = 0$, and $T = 300\,K$).

In Fig. 4 we show results for the thermoelectric coefficient vs chemical potential μ and density of the surface states N_T. The general trends we observed in Fig. 3 still hold for low chemical potentials. Increasing the chemical potential increases the electric conductivity and reduces the Seebeck coefficient. Increasing the density of the surface states leads to an increase of the barrier height and therefore reduces the electric conductivity and increases the Seebeck coefficient. The latter behavior can only be observed for low chemical potentials, because for larger chemical potentials a higher donor density N_D is required. A high donor density leads to a high effective screening of the trapped surface charge and therefore reduces the height and the width of the barrier (see Fig. 2).

In Fig. 5 the power factor for different chemical potentials and grain sizes is plotted. For low chemical potentials the power factor is reduced with increasing density of the surface states. For high chemical potentials there is no influence of the density of the surface states on the power factor. The grain size has only a small effect on the power factor. An appreciable enhancement of the power factor is not observed.

As already mentioned, the important quantity is not the power factor but the figure of merit. If the thermal conductivity is dominated by the lattice contribution the optimization of the power factor also optimizes the figure of merit. This is why we considered the power factor and not the figure of merit. Nevertheless, if the electric thermal conductivity κ_e is comparable to the lattice thermal conductivity, a reduction in the electric thermal conductivity can enhance the figure of merit. To estimate the order of magnitude of the electric thermal conductivity we show in Fig. 6 (top) the electric thermal conductivity for different chemical potentials vs the density of surface states N_T. For higher chemical potentials, κ_e is hardly influenced since a high chemical potential results in a low barrier. For low chemical potentials κ_e rapidly decreases with increasing N_T, but even without a barrier the absolute value of κ_e is much smaller than the smallest lattice thermal conductivities reported.[30]

Figure 6 (bottom) shows the Lorenz number [see Eq. (2)] for different chemical potentials as a function of N_T. The Lorenz

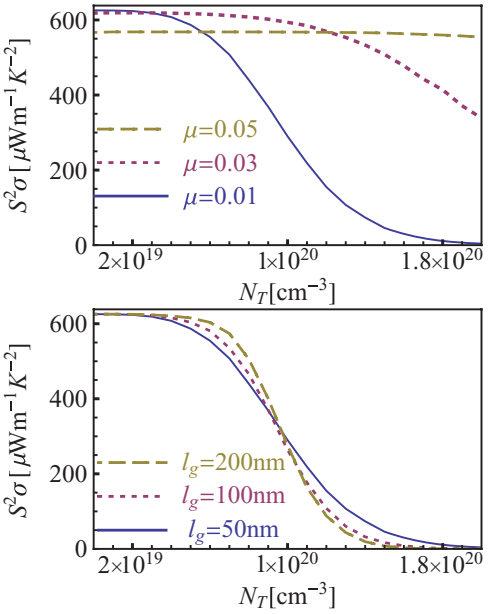

FIG. 5. (Color online) Top: Power factor vs density of the surface states N_T for different chemical potentials and a grain size $l_g = 100$ nm. Bottom: Power factor vs density of the surface states N_T for different grain sizes and a chemical potential $\mu = 0.1$.

number always increases with increasing N_T, but for low chemical potentials this effect is stronger. The Lorenz number increases because with increasing N_T the barrier increases as well. An increase of the barrier leads to a blocking of the cold electrons, which means that hot electrons are preferred to cross the barrier. Hence, on average, each charged particle carries more heat compared to the case without a barrier.

For the sake of completeness we also show the figure of merit for three different lattice thermal conductivities $\kappa_l =$

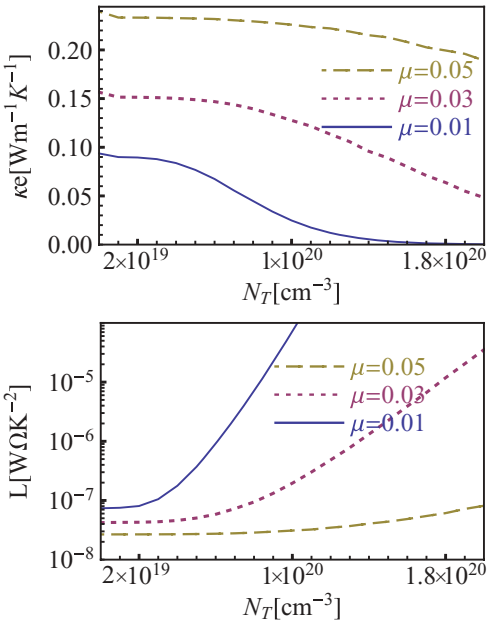

FIG. 6. (Color online) Top: Thermal conductivity of the electrons κ_e vs density of surface states N_T. Bottom: Lorenz number L vs density of surface states N_T.

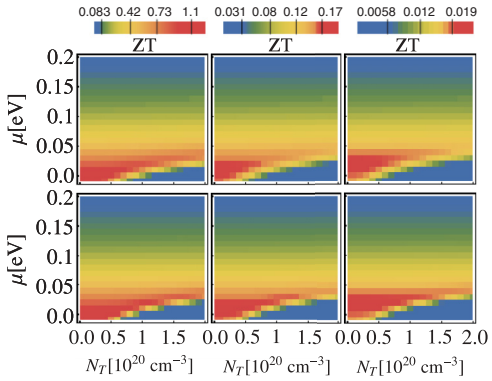

FIG. 7. (Color online) ZT vs chemical potential μ and density of surface states N_T for $\kappa_l = 0.1$ W/(mK) (left), $\kappa_l = 1$ W/(mK) (middle) and $\kappa_l = 10$ W/(mK) (right). Top: $l_g = 50$ nm. Bottom: $l_g = 200$ nm.

0.1,1,10 W/(mK) in Fig. 7. These values of κ_l are chosen to cover typical ranges of thermoelectric materials. In principle, the figure of merit shows the same behavior as the power factor, except that for low κ_l the figure of merit decreases earlier with increasing chemical potential μ than the power factor. The reason is that κ_e increases and hence reduces the figure of merit with increasing chemical potential. There is no qualitative difference between grain sizes of 50 nm and 200 nm.

IV. CONCLUSION

We employed a one-band effective mass model to capture the main effects in grain boundary structures. We showed for a simple model that an enhancement of the power factor can only be achieved when the barrier height is in the range of the chemical potential. For a realistic model these conditions could not be reproduced since a high chemical potential prevents a barrier due to screening effects. From this we conclude that an effective enhancement of the figure of merit at reasonable values of the chemical potential cannot be achieved by a double Schottky barrier. These results are contrary to general belief[5] and to results presented by Popescu *et al.*[9] They investigated the effect of energy filtering on grain boundaries and modeled the grain barriers using rectangular barriers, where they varied the height and width of the barrier independently from the other parameters. Therefore, they were able to obtain an enhancement in the power factor. In this paper we showed that the width and the height of the barrier depend on the chemical potential. If we employ the realistic model of the double Schottky barrier to describe the barrier formation due to charge accumulation in the grain boundaries an enhancement of the power factor is not observed for a wide range of realistic parameters. Nevertheless, we do not exclude that other energy-dependent scattering effects at grain boundaries can occur and that these effects can increase the power factor. To investigate these effects one has to perform *ab initio* calculations and simulate the grain boundary on an atomistic scale.

ACKNOWLEDGMENTS

We thank the Deutsche Forschungsgemeinschaft for supporting us in the framework of the priority program 1386 "Nanostructured thermoelectrics".

*christian.heiliger@physik.uni-giessen.de

[1] Yu. I. Ravich, in *CRC Handbook of Thermoelectrics*, edited by D. M. Rowe (CRC, Boca Raton, 1995), Chap. 7.
[2] G. A. Slack, in *CRC Handbook of Thermoelectrics*, edited by D. M. Rowe (CRC, Boca Raton 1995), p. 407.
[3] M. S. Dresselhaus, G. Chen1, M. Y. Tang, R. G. Yang, H. Lee, D. Z. Wang, Z. F. Ren, J.-P. Fleurial, and P. Gogna, Adv. Mater. **19**, 1043 (2007).
[4] D. Vashaee and A. Shakouri, Phys. Rev. Lett. **92**, 106103 (2004).
[5] D. L. Medlin and G. J. Snyder, Curr. Opin. Colloid Interface Sci. **14**, 226 (2009).
[6] S. V. Faleev and F. Leonard, Phys. Rev. B **77**, 214304 (2008).
[7] J. Martin, L. Wang, L. Chen, and G. S. Nolas, Phys. Rev. B **79**, 115311 (2009).
[8] B. Paul, A. Kumar V, and P. Banerji, J. Appl. Phys. **108**, 064322 (2010).
[9] A. Popescu, L. M. Woods, J. Martin, and G. S. Nolas, Phys. Rev. B **79**, 205302 (2009).
[10] J. M. O. Zide, D. Vashaee, Z. X. Bian, G. Zeng, J. E. Bowers, A. Shakouri, and A. C. Gossard, Phys. Rev. B **74**, 205335 (2006).
[11] J. P. Heremans, C. M. Thrush, and D. T. Morelli, J. Appl. Phys. **98**, 063703 (2005).
[12] J. P. Heremans, C. M. Thrush, and D. T. Morelli, Phys. Rev. B **70**, 115334 (2004).
[13] K. Kishimoto and T. Koyanagi, J. Appl. Phys. **92**, 2544 (2002).
[14] K. Kishimoto, K. Yamamoto, and T. Koyanagi, Jpn. J. Appl. Phys. **42**, 501 (2003).
[15] G. Joshi, H. Lee, Y. Lan, X. Wang, G. Zhu, D. Wang, R. W. Gould, D. C. Cuff, M. Y. Tang, M. S. Dresselhaus, G. Chen, and Z. Ren, Nano Lett. **8**, 4670 (2008).
[16] G. Homm, M. Piechotka, A. Kronenberger, A. Laufer, F. Gather, D. Hartung, C. Heiliger, B. K. Meyer, P. J. Klar, S. O. Steinmüller, and J. Janek, J. Electron. Mater. **39**, 1504 (2010).
[17] G. Homm, S. Petznick, F. Gather, T. Henning, C. Heiliger, B. K. Meyer, and P. J. Klar, J. Electron. Mater. **40**, 801 (2010).
[18] G. Homm, J. Teubert, T. Henning, P. J. Klar, and B. Szyszka, Phys. Status Solidi C **7**, 1602 (2010).
[19] R. Venkatasubramanian, E. Siivola, T. Colpitts, and B. O'Quinn, Nature (London) **413**, 597 (2001).
[20] J. Y. W. Seto, J. Appl. Phys. **46**, 5247 (1975).
[21] C. R. M. Grovenor, J. Phys. C **18**, 4079 (1985).
[22] G. D. Mahan, L. M. Levinson, and H. R. Philipp, J. Appl. Phys. **50**, 2799 (1979).
[23] A. J. Minnich, H. Lee, X. W. Wang, G. Joshi, M.S. Dresselhaus, Z. F. Ren, G. Chen, and D. Vashaee, Phys. Rev. B **80**, 155327 (2009).
[24] S. Datta, *Electronic Transport in Mesoscopic Systems* (Cambridge University Press, Cambridge, 1995).

[25]S. Datta, *Atom to Transistor* (Cambridge University Press, Cambridge, 2005).
[26]C. Heiliger, M. Czerner, B. Y. Yavorsky, I. Mertig, and M. D. Stiles, J. Appl. Phys. **103**, 07A709 (2008).
[27]M. Bachmann, M. Czerner, and C. Heiliger, J. Electron. Mater. **40**, 577 (2011).
[28]C. Jeong, R. Kim, M. Luisier, S. Datta, and M. Lundstrom, J. Appl. Phys. **107**, 023707 (2010).
[29]U. Sivan and Y. Imry, Phys. Rev. B **33**, 551 (1986).
[30]M. N. Touzelbaev, P. Zhou, R. Venkatasubramanian, and K. E. Goodson, J. Appl. Phys. **90**, 763 (2001).